Biochimica et Biophysica Acta 1823 (2012) 1856–1863

Contents lists available at SciVerse ScienceDirect

Biochimica et Biophysica Acta

journal homepage: www.elsevier.com/locate/bbamcr

Role of mitochondrial uncoupling protein 2 in cancer cell resistance to gemcitabine

Elisa Dalla Pozza, Claudia Fiorini, Ilaria Dando, Marta Menegazzi, Anna Sgarbossa, Chiara Costanzo, Marta Palmieri, Massimo Donadelli *

Department of Life and Reproduction Sciences, Biochemistry Section, University of Verona, Verona, Italy

ARTICLE INFO

Article history:
Received 11 May 2012
Received in revised form 6 June 2012
Accepted 7 June 2012
Available online 15 June 2012

Keywords:
Cancer
Gemcitabine
Uncoupling protein 2
Oxidative stress
Apoptosis
Resistance

ABSTRACT

Cancer cells exhibit an endogenous constitutive oxidative stress higher than that of normal cells, which renders tumours vulnerable to further reactive oxygen species (ROS) production. Mitochondrial uncoupling protein 2 (UCP2) can mitigate oxidative stress by increasing the influx of protons into the mitochondrial matrix and reducing electron leakage and mitochondrial superoxide generation. Here, we demonstrate that chemical uncouplers or UCP2 over-expression strongly decrease mitochondrial superoxide induction by the anticancer drug gemcitabine (GEM) and protect cancer cells from GEM-induced apoptosis. Moreover, we show that GEM IC_{50} values well correlate with the endogenous level of UCP2 mRNA, suggesting a critical role for mitochondrial uncoupling in GEM resistance. Interestingly, GEM treatment stimulates UCP2 mRNA expression suggesting that mitochondrial uncoupling could have a role also in the acquired resistance to GEM. Conversely, UCP2 inhibition by genipin or UCP2 mRNA silencing strongly enhances GEM-induced mitochondrial superoxide generation and apoptosis, synergistically inhibiting cancer cell proliferation. These events are significantly reduced by the addition of the radical scavenger *N*-acetyl-L-cysteine or MnSOD over-expression, demonstrating a critical role of the oxidative stress. Normal primary fibroblasts are much less sensitive to GEM/genipin combination. Our results demonstrate for the first time that UCP2 has a role in cancer cell resistance to GEM supporting the development of an anti-cancer therapy based on UCP2 inhibition associated to GEM treatment.

1. Introduction

Gemcitabine (2′,2′-difluoro-2′-deoxycytidine; GEM) is a critical component of therapeutic regimens in a broad range of malignancies, including pancreas, lung and bladder carcinomas, and represents one of the main options when combination therapy is employed. Despite more than 20 years of clinical use of GEM, its comprehensive mechanism of action on tumour cells is not fully elucidated. Currently, cancer research is focused on the identification of novel potential targets of response, the regulation of which may improve GEM antitumour activity.

Studies by our research group have recently demonstrated that the induction of reactive oxygen species (ROS) is one of the mechanisms of GEM antitumour action and that pancreatic adenocarcinoma cell lines with lower basal levels of ROS are more resistant to GEM compared to cells with higher ROS levels [1]. Compromised aerobic metabolism, nutrient deprivation, and host immune responses are among the main causes of the high ROS generation in cancer cells [2–4]. Ensuring that ROS levels remain in the non-toxic range is a continuous challenge for cancer cells, which invoke a suite of antioxidative defense strategies.

Uncoupling proteins (UCPs) belong to the superfamily of mitochondrial anion transporters [5,6]. In mammals, five different UCP homologues have been described, UCP 1–5, which have different levels of identity and different tissue distribution [7]. Several studies have shown that the antioxidant UCP2 is broadly over-expressed in cancer cells [8,9]. Increased UCP2 expression, associated with hypomethylation of its gene, was found in several hepatocellular cancer cell lines and suggested a role for epigenetic modifications in cancer UCP2 over-expression [8]. This feature may represent an adaptive mechanism developed by tumours to maintain ROS homeostasis [7,10]. UCP2 prevents mitochondrial superoxide generation, a major cause of the cellular oxidative damage [11], by increasing the proton flow into the matrix thus rendering the electron flow through the respiratory complexes more efficient [12,13]. Indeed, even slight depolarisation of the $\Delta\Psi m$ can diminish electron escape and reduce mitochondrial superoxide production [14,15].

Recently, tumour xenografts of UCP2-overexpressing colon cancer cells have been shown to be much more resistant to the topoisomerase I inhibitor CPT-11 as compared to control cells [16]. Moreover, Mailloux et al. demonstrated that the specific UCP2 inhibitor, genipin, was able to sensitise drug-resistant leukemia cells to anthracyclin [17], suggesting that UCP2 targeting may be a novel therapeutic strategy for cancer.

* Corresponding author at: Dept. of Life and Reproduction Sciences, Section of Biochemistry, University of Verona, Strada Le Grazie 8, 37134 Verona, Italy. Tel.: +39 045 8027281; fax: +39 045 8027170.
E-mail address: massimo.donadelli@univr.it (M. Donadelli).

0167-4889/$ – see front matter © 2012 Elsevier B.V. All rights reserved.
doi:10.1016/j.bbamcr.2012.06.007

Here, we have investigated for the first time the involvement of UCP2 gene regulation in the cell resistance to GEM and the antitumoural effect of GEM treatment associated to UCP2 inhibition. We used as cellular models tumours clinically treated with GEM, i.e. pancreas adenocarcinoma, non-small cell lung adenocarcinoma, and bladder carcinoma, and primary fibroblasts as normal control.

2. Materials and methods

2.1. Chemicals

Gemcitabine (2′,2′-difluoro-2′-deoxycytidine; GEM) was provided by Eli Lilly (Florence, Italy) and was solubilised in sterile water. Genipin (methyl-2-hydroxy-9-hydroxymethyl-3-oxabicyclonona-4,8-diene-5-carboxylate) and TTNPB (5,6,7,8-tetrahydro-5,5,8,8-tetramethyl-2-naphthalenyl-1-propenyl benzoic acid) were obtained from Sigma (Milan, Italy), solubilised in DMSO and stored at −80 °C until use. FCCP (4-trifluoro-methoxy-phenyl-hydrazone) was obtained from Sigma (Milan, Italy), solubilised in 95% ethanol and stored at −20 °C until use.

2.2. Cell culture

Pancreatic adenocarcinoma cell lines PaCa44, PaCa3, Panc1, CFPAC1, T3M4, and MiaPaCa2 were grown in RPMI 1640 supplemented with 2 mM glutamine, 10% FBS, and 50 μg/ml gentamicin sulfate (BioWhittaker, Lonza, Bergamo, Italy). Non-small cell lung adenocarcinoma cell line A549, bladder carcinoma RT112 cell line (kindly provided by Dr. Paco Francisco Real; Centro Nacional de Investigaciones Oncológicas; Madrid, Spain), and normal primary fibroblasts (PromoCell, PBI, Milan, Italy) were grown in DMEM supplemented with 2 mM glutamine, 10% FBS, and 50 μg/ml gentamicin sulfate (BioWhittaker, Lonza, Bergamo, Italy). All cell lines were incubated at 37 °C with 5% CO_2.

2.3. Cell proliferation assay

Cells were seeded in 96-well plates (5×10^3 cells/well), 24 h later treated with the various compounds and further incubated for the indicated times (see legends to figures). At the end of the treatments cells were stained with a Crystal Violet solution (Sigma, Milan, Italy). The dye was solubilised in PBS containing 1% SDS and measured photometrically (A595nm) to determine cell growth.

2.4. Drug combination studies

Drug combination studies were performed using the concentration ratio [GEM]:[genipin] = 1:500, which was chosen on the basis of GEM or genipin IC_{50} mean values. Taking into account the drug molar ratios, the in vitro ranges of concentration used were 20 nM → 2 μM for GEM and 10 μM → 1 mM for genipin. The Combination Index (CI) was calculated by the Chou–Talalay equation, which takes into account both the potency (IC_{50}) and the shape of the dose–effect curve [18,19], taking advantage of the CalcuSyn software (Biosoft, Cambridge, UK). The general equation for the classic isobologram is given by $CI = (D)1/(Dx)1 + (D)2/(Dx)2 + [(D)1\cdot(D)2]/[(Dx)1\cdot(Dx)2]$, where $(Dx)1$ and $(Dx)2$ in the denominators are the doses (or concentrations) for D1 (drug 1) and D2 (drug 2) alone that gives x% growth inhibition, whereas $(D)1$ and $(D)2$ in the numerators are the doses of drug 1 and drug 2 in combination that also inhibit *x*% cell growth (i.e., isoeffective). $CI<1$, $CI=1$, or $CI>1$ generally indicate synergistic, additive, or antagonistic effect, respectively. However, to obtain more compelling data, we decided to use a cut off for CI of 0.7 (as suggested by manufacturer directions), identifying a synergistic effect when CIs were smaller than 0.7. CI/effect curves represent the CI versus the fraction (0 → 1) of cells killed by drug combinations. The synergism percentage was obtained analysing CI/effect curve and measuring the CI values at each 0.05 fraction, i.e. 5% growth inhibition, of the antiproliferative effect.

2.5. Measurement of mitochondrial superoxide production

The non-fluorescent MitoSox Red probe (Molecular Probes, Invitrogen, Milan, Italy) was used to evaluate mitochondrial $O_2^{\bullet-}$ production. Briefly, cells were seeded in 96-well plates (5×10^3 cells/well) and, the day after, treated with the various compounds at the indicated concentration for 16 h. At the end of the treatments, cells were incubated in culture medium with 0.5 μM MitoSox probe at 37 °C for 15 min. Cells were washed with Hanks buffer (20 mM Hepes pH 7.2, 10 mM glucose, 118 mM NaCl, 4.6 mM KCl, and 1 mM $CaCl_2$) and fluorescence was measured by using a multimode plate reader (Ex 430 nm and Em 590 nm) (GENios Pro, Tecan, Milan, Italy). The probe is live-cell permeant and is rapidly and selectively targeted to the mitochondria where it becomes fluorescent after oxidation by $O_2^{\bullet-}$. The usage of 430 ± 35 nm of excitation wavelengths allowed us to selectively detect mitochondrial $O_2^{\bullet-}$ strongly reducing the recognition of other oxidants (e.g., $^{\cdot}OH$, $ONOO^{\cdot-}$) [20–22]. The values were normalised on cell proliferation by Crystal Violet assay.

2.6. RNA extraction and qPCR

Total RNA was extracted from cells using a highly denaturing guanidine-thiocyanate-containing buffer and RNeasy Mini spin columns (Qiagen, Milan, Italy). The concentration of purified RNA was determined measuring the absorbance at 260 nm with a NanoDrop 1000 spectrophotometer (Thermo Scientific, Milan, Italy). 1 μg of RNA was reverse transcribed using SuperScript® VILO cDNA Synthesis Kit (Invitrogen, Milan, Italy). Real time PCR analyses were performed with a QuantiTect SYBR Green PCR kit (Qiagen, Milan, Italy) and a Rotor-Gene™ 6000 (Corbett Research, Cambridge, UK) using the following primers: Hs_UCP2_1_SG QuantiTect Primer Assay for the UCP2 gene and Hs_RRN18S_1_SG QuantiTect Primer Assay (Qiagen, Milan, Italy) for 18S rRNA. The amplification conditions consisted in an initial step of 15 minutes at 95 °C to activate HotStarTaq DNA polymerase and 45 cycles of denaturation at 94 °C for 15 seconds, annealing at 55 °C for 30 seconds, and extension at 72 °C for 30 seconds.

2.7. Immunoblot analysis

Cells were harvested, washed in phosphate-buffered saline, and re-suspended in 50 mM Tris–HCl pH 7.5, 150 mM NaCl, 1% Triton X-100, 1 mM PMSF, and 1× protease inhibitor cocktail (Roche Diagnostic, Monza, Italy). After three freeze/thaw cycles and incubation on ice for 15 min, the lysate was centrifuged at 14,000 ×*g* for 10 min at 4 °C and the supernatant used for Western blot. Protein concentration was measured with the Bradford protein assay reagent (Pierce, Milan, Italy) using bovine serum albumin as a standard. Protein extracts (15 μg/lane for MnSOD or 35 μg/lane for PARP) were electrophoresed through a 12% (MnSOD) or 7.5% (PARP) SDS-polyacrylamide gel and electro-blotted onto PVDF membranes (Millipore, Milan, Italy). Membranes were then incubated overnight at 4 °C with blocking solution [5% low-fat milk in TBST (100 mM Tris pH 7.5, 0.9% NaCl, 0.1% Tween 20)] and probed for 1 h at room temperature with a mouse monoclonal anti-MnSOD antibody (1:2000 in blocking solution; Abcam, Cambridge, UK) or a rabbit monoclonal anti-PARP antibody (1:1000 in blocking solution; Cell Signaling, Milan, Italy). Horseradish peroxidase conjugated anti-mouse IgG (for MnSOD detection) or anti-rabbit IgG (for PARP detection) (1:8000 in blocking solution; Upstate Biotechnology, Milan, Italy) were used to detect specific proteins. Immunodetection was carried out using chemiluminescent substrates (Amersham Pharmacia Biotech, Milan, Italy) and recorded using a HyperfilmECL (Amersham Pharmacia Biotech). Ponceau S dye was used as control loading.

2.8. Apoptosis

Cells were seeded in 96-well plates (5×10^3 cells/well) and, the day after, treated with the various compounds at the indicated concentrations for 48 h. At the end of the treatment, cells were fixed with 2% paraformaldehyde in PBS at room temperature for 30 min, then washed twice with PBS and stained with annexinV/FITC (Bender MedSystem, Milan, Italy) in binding buffer (10 mM HEPES/NaOH pH 7.4, 140 mM NaOH, and 2.5 mM $CaCl_2$) for 10 min at room temperature in the dark. Finally, cells were washed with binding buffer solution and fluorescence was measured by using a multimode plate reader (Ex 485 nm and Em 535 nm) (GENios Pro, Tecan, Milan, Italy). The values were normalised on cell proliferation by Crystal Violet assay.

2.9. Transient transfection experiments

Exponentially growing cells were seeded at a density of 5×10^3 cells/well in 96-well plates for proliferation assays and at 2.5×10^5 cells/plate in 60 mm cell culture plates for protein extraction. Twenty-four hours later, transfections were carried out with a pCR3.1 expression vector containing the cDNA of human MnSOD (kindly provided by Dr. Akashi, National Institute of Radiological Sciences, Chiba, Japan) using TransIT-LT1 transfection reagent (Mirus, Tema Ricerca, Bologna, Italy) according to manufacturer. Cells transfected with the empty pCR3.1 vector were used as a control and behaved as the untransfected cells (data not shown). Cells were incubated for 24 h and then treated with GEM/genipin for the indicated periods.

UCP2 over-expression experiments were performed using a pCMV expression vector containing the human cDNA of UCP2 (OriGene Technologies, Rockville, MD) using TransIT-LT1 transfection reagent (Mirus, Tema Ricerca, Bologna, Italy). Cells transfected with the empty pCMV vector were used as a negative control (mock). Cells were incubated for 24 h and treated with GEM to evaluate the effect of UCP2 over-expression on GEM-induced cell growth inhibition and apoptosis.

2.10. siRNA transfections and UCP2 silencing

Exponentially growing cells were seeded at a density of 5×10^3 cells/well in 96-well plates for proliferation assays and at 2.5×10^5 cells/plate in 60 mm cell culture plates for RNA extraction. Twenty-four hours later, transfections were carried out with a specific small interfering (si) (5′-GCUAAAGUCCGGUUACAGATT-3′) RNA targeting UCP2 mRNA and a non-targeting (NT) siRNA (5′-CAGUCGCGUUUGCGACUGG-3′) purchased by Ambion Life Technologies (Monza MB, Italy). Cells were transfected with siRNAs at a final concentration of 200 nM using Transfectin for 72 h (Biorad, Milan, Italy).

2.11. Caspase activity

Cells were seeded in 96-well plates (5×10^3 cells/well) and, the day after, treated with the various compounds at the indicated concentrations for 48 h. At the end of the treatments, cells were incubated in culture medium with the fluorescent inhibitor/substrate of caspases FLICA (FAM-DEVD-FMK) (Molecular Probes, Invitrogen, Milan, Italy) for 60 min at 37 °C. FLICA reagent contains a carboxyfluorescein group (FAM) and a fluoromethyl ketone (FMK) moiety, which can react covalently with a cysteine residue. The recognition sequence aspartic acid–glutamic acid–valine–aspartic acid (DEVD) is specific for caspase-3 and -7. Cells were washed twice with wash buffer and fluorescence was measured by using a multimode plate reader (Ex 485 nm and Em 535 nm) (GENios Pro, Tecan, Milan, Italy). The values were normalised on cell proliferation by Crystal Violet assay.

2.12. Statistical analysis

ANOVA (post hoc Bonferroni) analysis was performed by GraphPad Prism 5 software. P value <0.05 was indicated as statistically significant.

3. Results

3.1. Mitochondrial uncoupling reduces GEM effect in cancer cells

To evaluate the impact of mitochondrial uncoupling on GEM effects, we treated cells with GEM in the absence or presence of FCCP, a known chemical uncoupler, TTNPB, a retinol compound able to activate UCP2 proton conductance [23,24], or UCP2 over-expression. Low concentrations of FCCP or TTNPB significantly protected cells from GEM-induced cell growth inhibition (Fig. 1A) and apoptosis (Fig. 1B), and prevented mitochondrial superoxide induction by GEM (Fig. 1C). In line with published data, Supplementary Fig. 1A and B shows that while low concentrations of FCCP determined a modest proliferative and anti-apoptotic effect, high concentrations were toxic to the cells. TTNPB treatment was instead slightly effective on cell proliferation at the higher concentrations tested (Supplementary Fig. 1C). Consistently, cell growth inhibition and apoptosis by GEM was significantly reduced by UCP2 over-

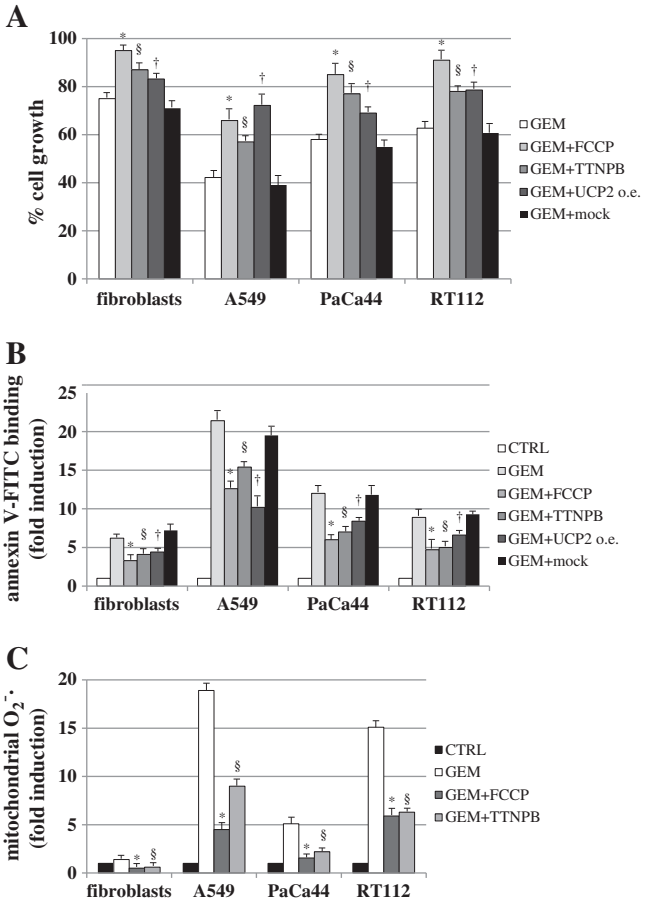

Fig. 1. Effects of GEM on cell growth (A), apoptosis (B), and mitochondrial superoxide production (C) in the absence or presence of FCCP, TTNPB, UCP2 over-expression or empty vector (mock). Cells were seeded in 96-well plates, incubated overnight, and treated with 1 μM GEM (48 h) alone or in the presence of 1 μM FCCP or 300 nM TTNPB for 48 h (A and B) or 16 h (C). UCP2 over-expression was performed transfecting cells with 100 ng pCMV-UCP2 vector or pCMV empty vector using TransIT-LT1 transfection reagent for 72 h (A and B). Cell proliferation was determined using the Crystal Violet colorimetric assay; apoptosis was analysed using the annexin V binding assay; mitochondrial superoxide production was determined using the MitoSox Red probe as described in Materials and methods. Values are the means (±SD) of three independent experiments each performed in triplicate. Statistical analysis: (*) $P<0.05$ GEM + FCCP vs GEM; (§) $P<0.05$ GEM + TTNPB vs GEM; (†) $P<0.05$ GEM + UCP2 o.e. vs GEM or GEM + mock.

expression (Fig. 1A and B). Cell transfection efficiency was assessed by cytofluorimetric analysis as representatively shown in Supplementary Fig. 2A and ranged between 30% and 45% (Supplementary Fig. 2B). The fold induction of UCP2 mRNA after pCMV-UCP2 or empty vector transfection was analysed using qRT-PCR and reported in Supplementary Fig. 3A.

To further investigate the involvement of UCP2 in the cellular resistance to GEM, we characterised a panel of six cell lines belonging to the same tumour type (human pancreatic adenocarcinoma) for UCP2 expression (Fig. 2A) and we found that the basal level of UCP2 mRNA well correlated with GEM IC_{50} values (Fig. 2B). Consistent with the antioxidant role of UCP2, the constitutive endogenous amount of mitochondrial superoxide inversely correlated with UCP2 mRNA level (Fig. 2C). Altogether, these data indicate that UCP2-mediated mitochondrial uncoupling has a critical role in intrinsic cancer resistance to GEM. Additionally, inasmuch as GEM was able to induce UCP2 mRNA expression in all cell lines tested (Fig. 3), we suggest a role of UCP2 induction also in the acquired cancer resistance to GEM.

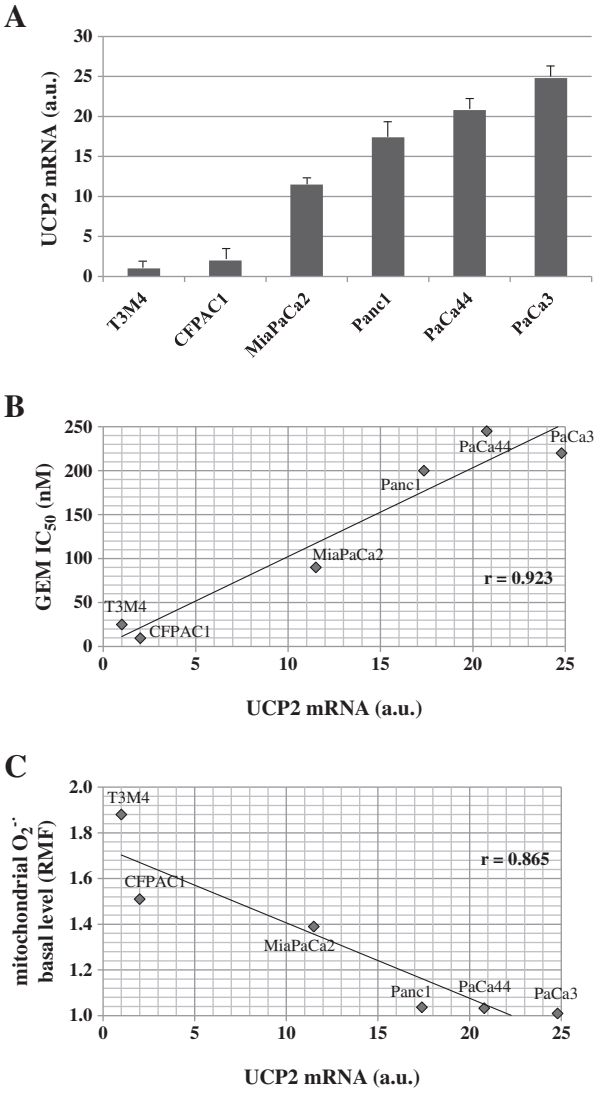

Fig. 2. Analysis of the constitutive expression of UCP2 mRNA in a panel of six pancreatic adenocarcinoma cell lines (A). Gene expression analysis of UCP2 was normalised to 18S rRNA and values are reported as arbitrary units (a.u.) calculated assigning the value of 1 to the pancreatic cancer cell line (T3M4) harbouring the lowest UCP2 mRNA level. Values are the means (±SD) of three independent experiments each performed in triplicate. Correlation between the constitutive expression of UCP2 mRNA and the GEM IC_{50} at 48 h (B) or the mitochondrial superoxide basal level (C). The MitoSox Red fluorescence intensity, corresponding to the level of mitochondrial superoxide production, is reported as relative mean fluorescence values (RMF). RMF is the ratio between fluorescence intensity of MitoSox treated versus untreated (autofluorescence) cells.

3.2. GEM treatment and UCP2 inhibition synergistically inhibit cancer cell proliferation

The antiproliferative effect of GEM in combination with genipin, a highly selective inhibitor of UCP2 [25], or with UCP2 siRNA was examined on three cancer cell lines (A549, PaCa44, and RT112) and normal fibroblasts. Both UCP2 inhibition by genipin or UCP2 silencing by siRNA in combination with GEM significantly increased cell growth inhibition as compared to single treatments in all cancer cell lines, but in fibroblasts (Fig. 4A and B). The efficiency of UCP2 silencing by siRNA targeting UCP2 mRNA or non-targeting (NT) siRNA was analysed using qRT-PCR and reported in Supplementary Fig. 3B.

To evaluate whether GEM in combination with the UCP2 inhibitor genipin determined a synergistic effect, we analysed cell growth inhibition curves by using the dedicated software CalcuSyn (see Materials and methods). Dose-dependent analyses performed at 48 h with different concentrations of GEM and/or genipin revealed that the combined setting induced a relevant percentage of antiproliferative synergism in cancer cells (53%, 62.5%, and 85.5%, for A549, PaCa44, and RT112 cell lines, respectively), which was instead modest (7.5%) in normal fibroblasts (Fig. 4C). Fig. 4D shows the isobologram curves of the combination index (CI) values versus the fraction (0→1) of cells killed by drug combination. The CI_{50} values were 0.43, 0.56, and 0.66 for A549, PaCa44, and RT112 cells, respectively, while it was 0.89 for normal fibroblasts (Table 1). Notably, a 2.3- up to 56.98-fold reduction in the IC_{50} of GEM and a 1.5- up to 711-fold reduction in the IC_{50} of genipin (DRI_{50}) were observed in combination settings compared to single treatments (Table 1).

To analyse the trend of the inhibitory effect over the time, we performed a time-dependent analysis of the antiproliferative activity following a 24 h single-step treatment with low concentrations of GEM and/or genipin. Fig. 4E shows that, at the sixth day, the combined treatment was able to significantly reduce proliferation of cancer cells, but that of fibroblasts, as compared to single treatments, with a growth ratio reduction versus untreated cells of 58%, 49.2%, and 53.8% for A549, PaCa44, and RT112 cell lines, respectively.

3.3. GEM treatment and UCP2 inhibition strongly induce mitochondrial superoxide production in cancer cells

In consideration of the described capability of UCP2 inhibition [7] or GEM treatment [26] to stimulate mitochondrial superoxide production in cancer cells, we investigated whether the association of GEM with genipin or UCP2 siRNA could enhance mitochondrial superoxide

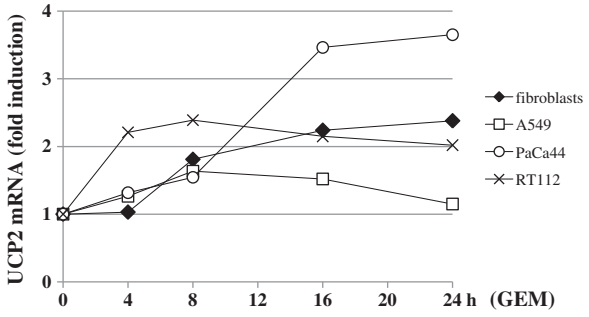

Fig. 3. Effect of GEM on UCP2 gene expression. Cells were treated with 1 μM GEM for the indicated time periods. Real-time PCR for UCP2 was performed as described in Materials and methods. Gene expression analysis of UCP2 was normalised to 18S rRNA. Values are the means of triplicate samples from three independent experiments (±S.D.). Statistical analysis: UCP2 gene was significantly induced ($P<0.05$) in RT112 cell line at 4 h, in all four cell lines at 8 h and 16 h, in fibroblasts, RT112, and PaCa44 cell lines at 24 h.

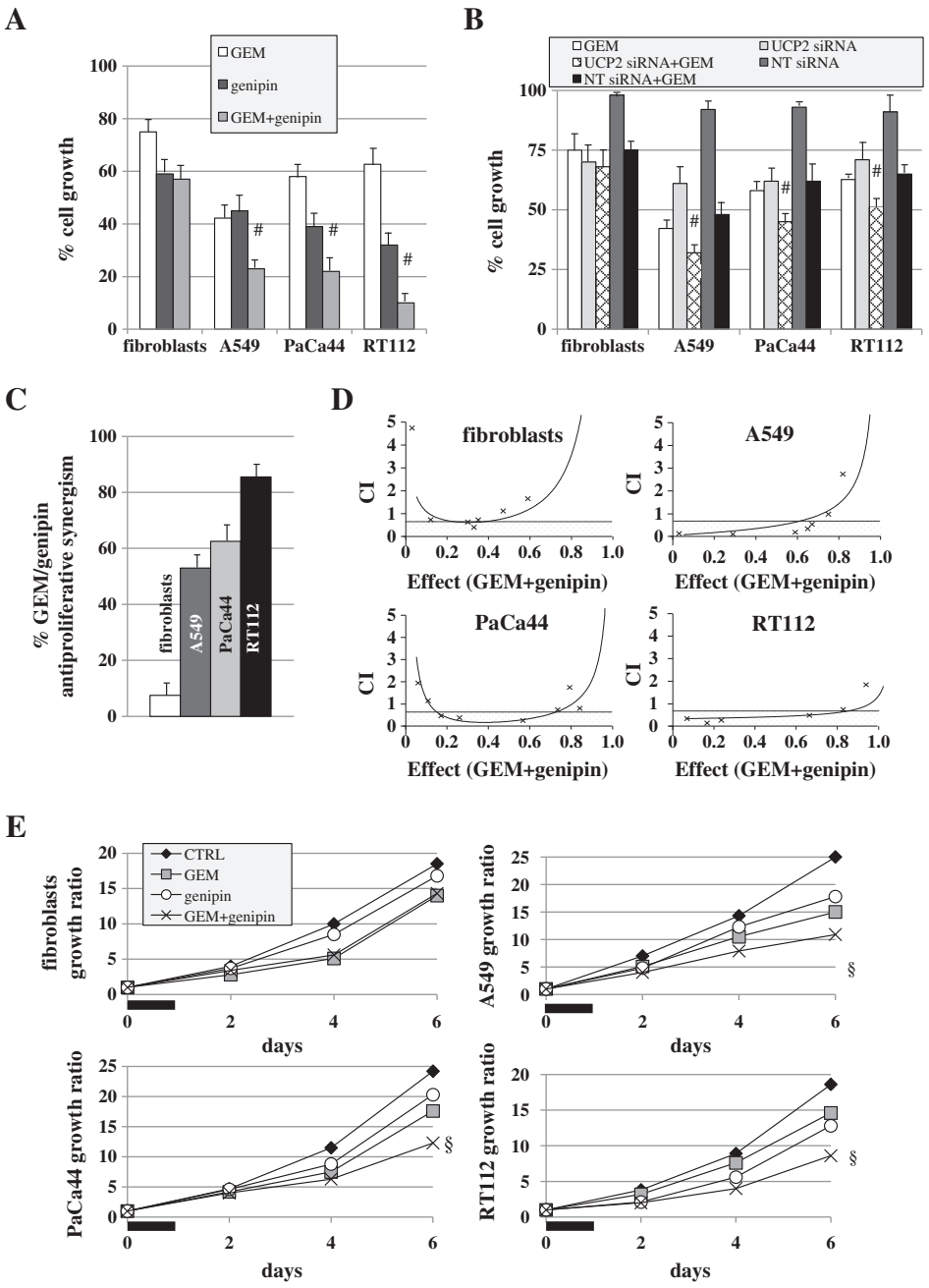

Fig. 4. Effects of GEM and UCP2 inhibition on cell growth. (A) Cells were seeded in 96-well plates, incubated overnight, and treated with 1 μM GEM and/or 500 μM genipin for 48 h. Cell proliferation was determined using the Crystal Violet colorimetric assay. Values are the means (± SD) of three independent experiments each performed in triplicate. Statistical analysis: (#) $P<0.05$ GEM + genipin vs GEM or genipin. (B) Cells were seeded in 96-well plates, incubated overnight, and treated with 1 μM GEM for 48 h and/or 200 nM UCP2 siRNA or NT siRNA for 72 h. Cell proliferation was determined using the Crystal Violet colorimetric assay. Values are the means (± SD) of three independent experiments each performed in triplicate. Statistical analysis: (#) $P<0.05$ GEM + UCP2 siRNA vs GEM or NT siRNA + GEM or UCP2 siRNA. (C) Quantitative analysis of the synergistic cell growth inhibition (CI<0.7) by the combined treatment GEM + genipin, as described in Materials and methods. The mean values (± SD) of the percentages of synergism are shown for each cell line. (D) CI/fractional effect curves for fibroblasts and cancer cell lines (A549, PaCa44, and RT112). A 1:500 molar ratio of GEM:genipin has been evaluated as described in Materials and methods. The figure shows the fractional effects versus the different CIs. The fractional effect is the % of cell growth inhibition given by each combination of the two drugs maintaining the same molar ratio (1:500) and increasing drug concentrations. This value is represented on the *X* axis of the curve. CI values obtained by the same combinations are reported on the *Y* axis. CIs below 0.7 indicate synergistic conditions. (E) Cells were seeded in 96-well plates and incubated overnight. The compounds were added at low concentrations for 24 h: 100 nM GEM and/or 50 μM genipin. The values on the *X* axis correspond to the days after the beginning of the treatments at which cell growth was analysed. The growth ratio on the *Y* axis was obtained by dividing the absorbance of untreated or treated cell lines by the mean absorbance of each cell line measured at time 0 and corresponds to the folds of cell proliferation increase from the beginning of cell treatments. The bar corresponds to the time period relative to the presence of GEM and/or genipin in culture medium (24 h) after which cells were maintained in drug-free medium. Values are the means of triplicate samples from three independent experiments. Statistical analysis: (§) $P<0.05$ GEM + genipin vs GEM or genipin.

production. Fig. 5A shows that in cancer cells GEM + genipin determined an induction of mitochondrial superoxide much higher than that induced by single compounds. Notably, in fibroblasts, the intensity of mitochondrial superoxide induction was very low and its enhancement by drug combination did not occur. Similar results were obtained after UCP2 silencing in combination with GEM treatment (Fig. 5B). As expected, mitochondrial superoxide induction by GEM + genipin combined treatment was significantly reduced by the radical scavenger

Table 1
Combination Index (CI) and Dose Reduction Index (DRI) values for GEM and genipin combination.

CELL LINES	CI_{50}	DRI_{50}	*r*
Fibroblasts	0.89	GEM: 4.27 genipin: 1.52	0.92
A549	0.43	GEM: 2.33 genipin: 711.53	0.86
PaCa44	0.56	GEM: 8.93 genipin: 2.25	0.98
RT112	0.66	GEM: 56.98 genipin: 1.55	0.94

CI_{50} was calculated for 50% cell growth inhibition in the combined treatment by isobologram analyses performed with the CalcuSyn software. DRI_{50} represents the folds of dose reduction to obtain 50% cell growth inhibition in combination setting as compared to each drug alone.

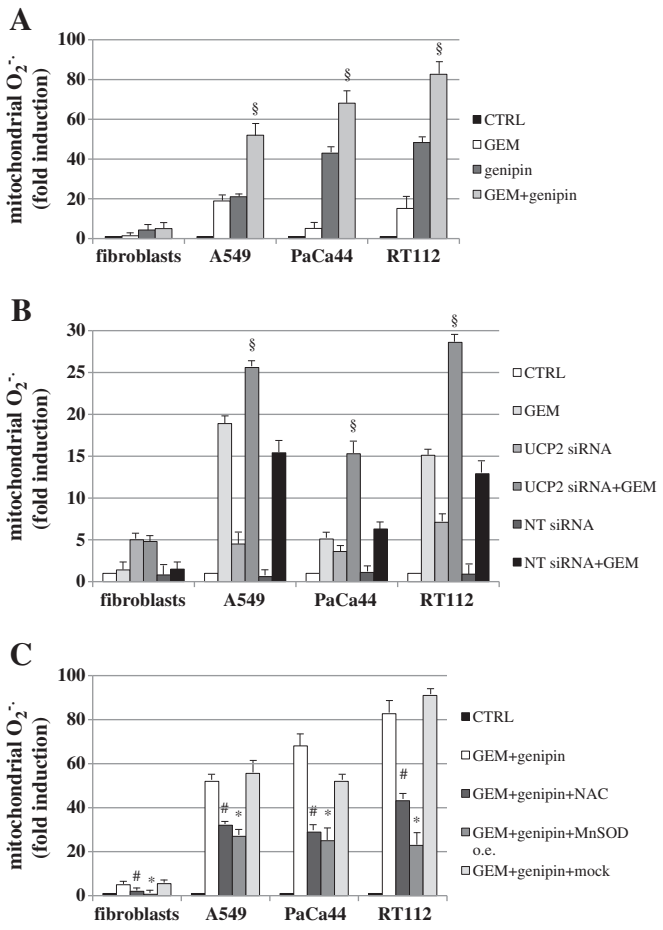

Fig. 5. Effects of GEM and UCP2 inhibition on mitochondrial superoxide production. (A) Cells were seeded in 96-well plates, incubated overnight, and treated with 1 μM GEM and/or 500 μM genipin for 16 h. The fluorescence intensity of the MitoSox Red probe, corresponding to the level of mitochondrial superoxide production, was measured by using a multimode plate reader, as described in Materials and methods. Values are the means (±SD) of three independent experiments each performed in triplicate. Statistical analysis: (§) $P<0.05$ GEM + genipin vs GEM or genipin. (B) Cells were seeded in 96-well plates, incubated overnight, and treated with 200 nM UCP2 or NT siRNAs for 72 h and/or 1 μM GEM for the last 16 h. The fluorescence intensity of the MitoSox Red probe, corresponding to the level of mitochondrial superoxide production, was measured by using a multimode plate reader, as described in Materials and methods. Values are the means (±SD) of three independent experiments each performed in triplicate. Statistical analysis: (§) $P<0.05$ GEM + UCP2 siRNA vs GEM or NT siRNA + GEM or UCP2 siRNA. (C) Cells were seeded in 96-well plates, incubated overnight, and treated with 1 μM GEM and/or 500 μM genipin for 16 h, in the absence or presence of 10 mM NAC or MnSOD over-expression (o.e.). Values are the means (±SD) of three independent experiments each performed in triplicate. Statistical analysis: (#) $P<0.05$ GEM + genipin + NAC vs GEM + genipin; (*) $P<0.05$ GEM + genipin + MnSOD o.e. vs GEM + genipin or GEM + genipin + mock.

N-acetyl-L-cysteine (NAC) or by MnSOD overexpression (Fig. 5C). The relative intensity of MnSOD before and after transfection with MnSOD expression vector or empty vector was analysed and shown in Supplementary Fig. 4A and B.

3.4. GEM treatment and UCP2 inhibition strongly induce ROS-mediated apoptosis in cancer cells

Fluorescence analysis using annexinV-FITC assay shows that in cancer cells both GEM + genipin and GEM + UCP2 siRNA significantly increased apoptosis induced by single treatments (Fig. 6A and B). In normal fibroblasts, apoptosis induction by single treatments was lower than in cancer cells and was not enhanced by the combined treatments. Fig. 6C shows that GEM/genipin-induced apoptosis and cell growth inhibition were significantly reduced by the radical scavenger NAC or MnSOD over-expression. These data together with those reported in Fig. 5 indicate that oxidative stress plays a critical role in GEM + genipin antiproliferative effect.

To further analyse the apoptotic pathway, we evaluated caspase activities and PARP cleavage after treatment with GEM and/or genipin. In line with data reported in Fig. 6, caspase-3 and-7 activities (Fig. 7A) and PARP cleavage (Fig. 7B) were higher in the combined treatment as compared to single settings. Notably, both these events were much less intense in normal fibroblasts than in cancer cells.

Representative images of A549 cells stained with Hoechst to indentify nuclei, FLICA to evaluate caspase-3 and -7 activities, or propidium iodide to analyse nuclear membrane damage were reported in Supplementary Fig. 5. In agreement with the previous data reporting the involvement of massive apoptotic cell death, GEM + genipin combination rendered cells much more positive to FLICA and propidium iodide staining as compared to single treatments.

4. Discussion

The pyrimidine nucleoside analog GEM is one of the most safe and employed drugs against a variety of solid tumours. Our research group had previously demonstrated that oxidative stress plays a role in pancreatic adenocarcinoma cell growth inhibition by GEM [1,26,27]. However, the clinical efficiency of GEM treatment is seriously impaired by tumour-related mechanisms of cell resistance [28–30]. In the present study, we have elucidated for the first time the role of UCP2-mediated mitochondrial uncoupling in cancer cell response to GEM. The cellular models chosen (pancreatic adenocarcinoma, non-small cell lung adenocarcinoma, and bladder carcinoma) constitute tumour types whose chemotherapeutic standard protocol is planned on GEM. We demonstrate that the response of cancer cells to GEM is significantly reduced by the mitochondrial uncoupling inducers FCCP or TTNPB, or by UCP2 over-expression; on the contrary, it is strongly enhanced following UCP2 silencing by siRNA or UCP2 inhibition by genipin, a highly selective inhibitor of UCP2-mediated proton leakage [25], via an oxidative stress-dependent mechanism. In a panel of six pancreatic adenocarcinoma cell lines, we report that increasing expression levels of UCP2 mRNA correlate directly with the GEM IC_{50} values and inversely with the constitutive level of endogenous mitochondrial superoxide. Altogether, these data and the observation that the UCP2 gene can be induced by GEM demonstrate that the antioxidant effect of the mitochondrial uncoupling by UCP2 plays a critical role in cancer cell resistance to GEM.

Besides UCP2 activation by superoxide ions and lipid peroxidation products [11], it has been reported that the levels of UCP proteins in tissues and cells is mainly regulated at the transcriptional level [31,32]. Here, we show that UCP2 mRNA is induced by GEM, although the identification of the precise mechanisms of this induction needs further investigation. Although GEM induces UCP2, the overall effect of GEM in the redox status of the cell leans towards a pro-oxidant outcome. Some authors have reported that GEM can generate ROS

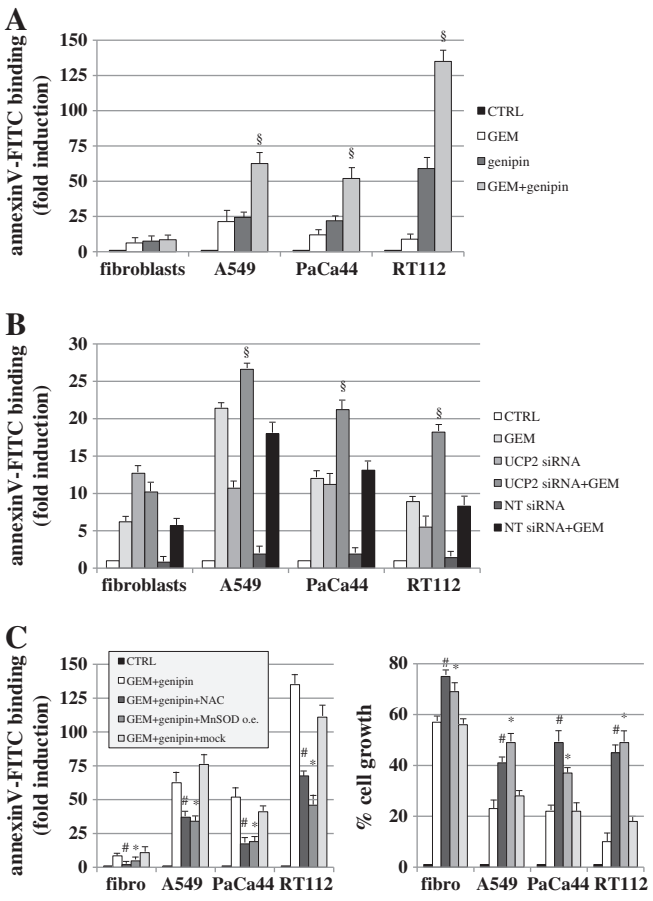

Fig. 6. Effects of GEM and UCP2 inhibition on apoptosis in the absence or presence of NAC or MnSOD over-expression. (A) Cells were seeded in 96-well plates, incubated overnight, and treated with 1 μM GEM and/or 500 μM genipin for 48 h. Apoptosis, corresponding to the level of annexinV-FITC binding to the cells, was measured by using a multimode plate reader, as described in Materials and methods. Values are the means (±SD) of three independent experiments each performed in triplicate. Statistical analysis: (§) $P<0.05$ GEM + genipin vs GEM or genipin. (B) Cells were seeded in 96-well plates, incubated overnight, and treated with 1 μM GEM for 48 h and/or 200 nM UCP2 siRNA or NT siRNA for 72 h. Apoptosis was analysed by the annexinV-FITC binding assay. Values are the means (±SD) of three independent experiments each performed in triplicate. Statistical analysis: (§) $P<0.05$ GEM + UCP2 siRNA vs GEM or NT siRNA + GEM or UCP2 siRNA. (C) Cells were seeded in 96-well plates, incubated overnight, and treated with 1 μM GEM and/or 500 μM genipin for 48 h, in the absence or presence of 10 mM NAC or MnSOD over-expression. Fold induction of annexinV-FITC binding or the percentage of cell growth relative to control (Crystal Violet assay) was measured. Values are the means (±SD) of three independent experiments each performed in triplicate. Statistical analysis: (#) $P<0.05$ GEM + genipin + NAC vs GEM + genipin; (*) $P<0.05$ GEM + genipin + MnSOD o.e. vs GEM + genipin or GEM + genipin + mock.

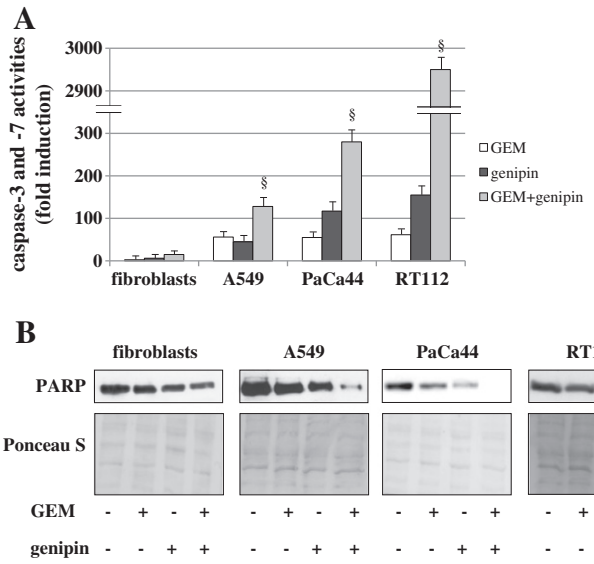

Fig. 7. Effects of GEM and/or genipin on down-stream caspase activities and PARP cleavage. (A) Cells were seeded in 96-well plates, incubated overnight, and treated with 1 μM GEM and/or 500 μM genipin for 48 h. The FLICA fluorescence intensity, corresponding to the level of caspase-3 and -7 activities was measured by using a multimode plate reader, as described in Materials and methods. Values are the means (±SD) of three independent experiments each performed in triplicate. Statistical analysis: (§) $P<0.05$ GEM + genipin vs GEM or genipin. (B) Western blot analysis of PARP after treatment with 1 μM GEM and/or 500 μM genipin for 48 h. Ponceau S staining was used as control loading.

via acid sphingomyelinase activation or neutral ceramidase inhibition with subsequent ceramide production [33,34], which directly affects the mitochondrial electron transport chain [35]. Since mitochondrial uncoupling can strongly decrease mitochondrial superoxide production, we tried to further increase GEM-induced oxidative stress by UCP2-mediated uncoupling inhibition. We report here that GEM is able to induce UCP2 mRNA and mitochondrial superoxide, which in turn is a main activator of UCP2 proton conductance [11], suggesting that GEM acts as a mitochondrial uncoupling activator by at least two different mechanisms. Genipin treatment or UCP2 siRNA strongly synergise with GEM in cancer cell growth inhibition and apoptosis. These events are mediated by ROS production as revealed by the strong enhancement of mitochondrial superoxide production in the combined treatment relative to single treatments and by the observation that mitochondrial superoxide production and apoptosis induction show a similar trend. Furthermore, we report that mitochondrial superoxide production, apoptosis and cell growth inhibition by GEM/genipin are, at least partially, preventable by the addition of the radical scavenger NAC or by over-expression of MnSOD, one of the main antioxidant enzymes located into mitochondria. The failure to totally inhibit GEM/genipin-mediated oxidative stress could lie in the intrinsic cytotoxicity of NAC when used at higher concentrations (data not shown) or in the relatively low percentage of MnSOD transfected cells, ranging between 30% and 45% (see Supplementary Fig. 2). Interestingly, mitochondrial superoxide production, apoptosis, and cell growth are only slightly affected by GEM/genipin or GEM/UCP2 siRNA treatments in normal primary fibroblasts. These results can be explained by the observation that cancer cells generally have an altered antioxidant defence system, as compared to normal cells, a feature that represents a specific vulnerability of tumours [36] and can be selectively targeted by pro-oxidant chemotherapeutics [4,26]. Although UCP2 inhibition by genipin increases the sensitivity of cancer cells to GEM, our data on normal fibroblasts indicate that further efforts need to be addressed to identify low-toxic UCP2 inhibitors. Future in vivo experiments will be performed to definitely support UCP2 inhibition as a successful anticancer strategy to enhance the therapeutic efficiency of GEM.

5. Conclusions

In summary, we have demonstrated for the first time that GEM induces UCP2 mRNA and that mitochondrial uncoupling by UCP2 is a mechanism of cancer cell resistance to GEM. We conclude that: i) the basal level of mitochondrial superoxide is critical for the response to GEM; ii) the basal level of mitochondrial superoxide is, at least in part, determined by the expression level of UCP2; iii) UCP2 endogenous expression could represent a potential predictive biomarker of cancer resistance to GEM; iv) UCP2 can be considered an efficient molecular target to selectively inhibit cancer cell proliferation in combined chemotherapeutic setting with GEM.

Supplementary data to this article can be found online at http://dx.doi.org/10.1016/j.bbamcr.2012.06.007.

Acknowledgments

We thank Dr. Akashi (National Institute of Radiological Sciences, Chiba, Japan) and Dr. Real (Centro Nacional de Investigaciones Oncológicas; Madrid, Spain) who kindly provided us with the expression vector for the human MnSOD and with the bladder carcinoma RT112 cell line, respectively. This work was supported by Associazione Italiana Ricerca Cancro (AIRC), Milan, Italy; Fondazione CariPaRo, Padova, Italy; Joint Project of University of Verona, Verona, Italy; Ministero dell'Istruzione, dell'Università e della Ricerca (MIUR), Rome, Italy.

References

[1] M. Donadelli, C. Costanzo, S. Beghelli, M.T. Scupoli, M. Dandrea, A. Bonora, P. Piacentini, A. Budillon, M. Caraglia, A. Scarpa, M. Palmieri, Synergistic inhibition of pancreatic adenocarcinoma cell growth by trichostatin A and gemcitabine, Biochim. Biophys. Acta 1773 (2007) 1095–1106.
[2] R.J. DeBerardinis, J.J. Lum, G. Hatzivassiliou, C.B. Thompson, The biology of cancer: metabolic reprogramming fuels cell growth and proliferation, Cell Metab. 7 (2008) 11–20.
[3] H. Kitano, Cancer as a robust system: implications for anticancer therapy, Nat. Rev. Cancer 4 (2004) 227–235.
[4] I. Muller, D. Niethammer, G. Bruchelt, Anthracycline-derived chemotherapeutics in apoptosis and free radical cytotoxicity (Review), Int. J. Mol. Med. 1 (1998) 491–494.
[5] O. Boss, P. Muzzin, J.P. Giacobino, The uncoupling proteins, a review, Eur. J. Endocrinol. 139 (1998) 1–9.
[6] C. Fleury, D. Sanchis, The mitochondrial uncoupling protein-2: current status, Int. J. Biochem. Cell Biol. 31 (1999) 1261–1278.
[7] G. Baffy, Uncoupling protein-2 and cancer, Mitochondrion 10 (2010) 243–252.
[8] M.V. Carretero, L. Torres, U. Latasa, E.R. Garcia-Trevijano, J. Prieto, J.M. Mato, M.A. Avila, Transformed but not normal hepatocytes express UCP2, FEBS Lett. 439 (1998) 55–58.
[9] M. Horimoto, M.B. Resnick, T.A. Konkin, J. Routhier, J.R. Wands, G. Baffy, Expression of uncoupling protein-2 in human colon cancer, Clin. Cancer Res. 10 (2004) 6203–6207.
[10] M.E. Harper, A. Antoniou, E. Villalobos-Menuey, A. Russo, R. Trauger, M. Vendemelio, A. George, R. Bartholomew, D. Carlo, A. Shaikh, J. Kupperman, E.W. Newell, I.A. Bespalov, S.S. Wallace, Y. Liu, J.R. Rogers, G.L. Gibbs, J.L. Leahy, R.E. Camley, R. Melamede, M.K. Newell, Characterization of a novel metabolic strategy used by drug-resistant tumor cells, FASEB J. 16 (2002) 1550–1557.
[11] M.D. Brand, C. Affourtit, T.C. Esteves, K. Green, A.J. Lambert, S. Miwa, J.L. Pakay, N. Parker, Mitochondrial superoxide: production, biological effects, and activation of uncoupling proteins, Free Radic. Biol. Med. 37 (2004) 755–767.
[12] M.D. Brand, T.C. Esteves, Physiological functions of the mitochondrial uncoupling proteins UCP2 and UCP3, Cell Metab. 2 (2005) 85–93.
[13] G. Mattiasson, P.G. Sullivan, The emerging functions of UCP2 in health, disease, and therapeutics, Antioxid. Redox Signal. 8 (2006) 1–38.
[14] B. Chance, H. Sies, A. Boveris, Hydroperoxide metabolism in mammalian organs, Physiol. Rev. 59 (1979) 527–605.
[15] J.F. Turrens, Mitochondrial formation of reactive oxygen species, J. Physiol. 552 (2003) 335–344.
[16] Z. Derdak, N.M. Mark, G. Beldi, S.C. Robson, J.R. Wands, G. Baffy, The mitochondrial uncoupling protein-2 promotes chemoresistance in cancer cells, Cancer Res. 68 (2008) 2813–2819.
[17] R.J. Mailloux, C.N. Adjeitey, M.E. Harper, Genipin-induced inhibition of uncoupling protein-2 sensitizes drug-resistant cancer cells to cytotoxic agents, PLoS One 5 (2010) e13289.
[18] F. Bruzzese, E. Di Gennaro, A. Avallone, S. Pepe, C. Arra, M. Caraglia, P. Tagliaferri, A. Budillon, Synergistic antitumor activity of epidermal growth factor receptor tyrosine kinase inhibitor gefitinib and IFN-alpha in head and neck cancer cells in vitro and in vivo, Clin. Cancer Res. 12 (2006) 617–625.
[19] T.C. Chou, P. Talalay, Quantitative analysis of dose–effect relationships: the combined effects of multiple drugs or enzyme inhibitors, Adv. Enzyme Regul. 22 (1984) 27–55.
[20] B. Kalyanaraman, V. Darley-Usmar, K.J. Davies, P.A. Dennery, H.J. Forman, M.B. Grisham, G.E. Mann, K. Moore, L.J. Roberts II, H. Ischiropoulos, Measuring reactive oxygen and nitrogen species with fluorescent probes: challenges and limitations, Free Radic. Biol. Med. 52 (2012) 1–6.
[21] K.M. Robinson, M.S. Janes, J.S. Beckman, The selective detection of mitochondrial superoxide by live cell imaging, Nat. Protoc. 3 (2008) 941–947.
[22] K.M. Robinson, M.S. Janes, M. Pehar, J.S. Monette, M.F. Ross, T.M. Hagen, M.P. Murphy, J.S. Beckman, Selective fluorescent imaging of superoxide in vivo using ethidium-based probes, Proc. Natl. Acad. Sci. U. S. A. 103 (2006) 15038–15043.
[23] S. Krauss, C.Y. Zhang, B.B. Lowell, A significant portion of mitochondrial proton leak in intact thymocytes depends on expression of UCP2, Proc. Natl. Acad. Sci. U. S. A. 99 (2002) 118–122.
[24] E. Rial, M. Gonzalez-Barroso, C. Fleury, S. Iturrizaga, D. Sanchis, J. Jimenez-Jimenez, D. Ricquier, M. Goubern, F. Bouillaud, Retinoids activate proton transport by the uncoupling proteins UCP1 and UCP2, EMBO J. 18 (1999) 5827–5833.
[25] C.Y. Zhang, L.E. Parton, C.P. Ye, S. Krauss, R. Shen, C.T. Lin, J.A. Porco Jr., B.B. Lowell, Genipin inhibits UCP2-mediated proton leak and acutely reverses obesity- and high glucose-induced beta cell dysfunction in isolated pancreatic islets, Cell Metab. 3 (2006) 417–427.
[26] E. Dalla Pozza, M. Donadelli, C. Costanzo, T. Zaniboni, I. Dando, M. Franchini, S. Arpicco, A. Scarpa, M. Palmieri, Gemcitabine response in pancreatic adenocarcinoma cells is synergistically enhanced by dithiocarbamate derivatives, Free Radic. Biol. Med. 50 (2011) 926–933.
[27] M. Donadelli, I. Dando, T. Zaniboni, C. Costanzo, E. Dalla Pozza, M.T. Scupoli, A. Scarpa, S. Zappavigna, M. Marra, A. Abbruzzese, M. Bifulco, M. Caraglia, M. Palmieri, Gemcitabine/cannabinoid combination triggers autophagy in pancreatic cancer cells through a ROS-mediated mechanism, Cell Death Dis. 2 (2011) e152.
[28] E. Mini, S. Nobili, B. Caciagli, I. Landini, T. Mazzei, Cellular pharmacology of gemcitabine, Ann. Oncol. 17 (Suppl. 5) (2006) v7–v12.
[29] A.M. Bergman, H.M. Pinedo, G.J. Peters, Determinants of resistance to 2′,2′-difluorodeoxycytidine (gemcitabine), Drug Resist. Updat. 5 (2002) 19–33.
[30] G. Hu, F. Li, K. Ouyang, F. Xie, X. Tang, K. Wang, S. Han, Z. Jiang, M. Zhu, D. Wen, X. Qin, L. Zhang, Intrinsic gemcitabine resistance in a novel pancreatic cancer cell line is associated with cancer stem cell-like phenotype, Int. J. Oncol. 40 (2012) 798–806.
[31] H. Oberkofler, K. Klein, T.K. Felder, F. Krempler, W. Patsch, Role of peroxisome proliferator-activated receptor-gamma coactivator-1alpha in the transcriptional regulation of the human uncoupling protein 2 gene in INS-1E cells, Endocrinology 147 (2006) 966–976.
[32] F. Villarroya, R. Iglesias, M. Giralt, PPARs in the control of uncoupling proteins gene expression, PPAR Res. 2007 (2007) 74364.
[33] C.A. Dumitru, I.E. Sandalcioglu, M. Wagner, M. Weller, E. Gulbins, Lysosomal ceramide mediates gemcitabine-induced death of glioma cells, J. Mol. Med. 87 (2009) 1123–1132.
[34] D.E. Modrak, E. Leon, D.M. Goldenberg, D.V. Gold, Ceramide regulates gemcitabine-induced senescence and apoptosis in human pancreatic cancer cell lines, Mol. Cancer Res. 7 (2009) 890–896.
[35] C. Garcia-Ruiz, A. Colell, M. Mari, A. Morales, J.C. Fernandez-Checa, Direct effect of ceramide on the mitochondrial electron transport chain leads to generation of reactive oxygen species. Role of mitochondrial glutathione, J. Biol. Chem. 272 (1997) 11369–11377.
[36] A. Laurent, C. Nicco, C. Chereau, C. Goulvestre, J. Alexandre, A. Alves, E. Levy, F. Goldwasser, Y. Panis, O. Soubrane, B. Weill, F. Batteux, Controlling tumor growth by modulating endogenous production of reactive oxygen species, Cancer Res. 65 (2005) 948–956.